

Physics Issues in the Design of Low Aspect-Ratio, High- β , Quasi-Axisymmetric Stellarators

M.C. Zarnstorff¹, L.A. Berry², A. Boozer³, A. Brooks¹, W.A. Cooper⁴, M. Drevlak⁵, E. Fredrickson¹, G.-Y. Fu¹, R. Goldston¹, R. Hatcher¹, S. Hirshman², W. Houlberg², S. Hudson¹, M. Isaev⁶, C. Kessel¹, L.-P. Ku¹, E. Lazarus², J. Lewandowski¹, Z. Lin¹, J. Lyon², R. Majeski¹, P. Merkel⁵, M. Mikhailov⁶, D. Mikkelsen¹, W. Miner⁷, D. Monticello¹, H. Mynick¹, G.H. Neilson¹, B.E. Nelson², C. Nuehrenberg⁵, N. Pomphrey¹, M. Redi¹, W. Reiersen¹, A. Reiman¹, P. Rutherford¹, R. Sanchez⁸, J. Schmidt¹, D. Spong², S. Subbotin⁶, P. Strand², D. Strickler², P. Valanju⁷, and R.B. White¹

¹Princeton Plasma Physics Laboratory, Princeton, NJ 08543 USA

²Oak Ridge National Laboratory, Oak Ridge, TN 37831 USA

³Columbia University, New York, NY 10027 USA

⁴Ecole Polytechnique Federale de Lausanne, Lausanne, Switzerland

⁵Max Planck Institute for Plasma Physics, Greifswald, Germany

⁶Kurchatov Institute, Moscow, Russia

⁷University of Texas at Austin, Austin, TX 78712 USA

⁸Universidad Carlos III de Madrid, Spain

email contact of first author: zarnstorff@pppl.gov

Abstract. Compact stellarators have the potential to combine the best features of the stellarator and the advanced tokamak, offering steady state operation without current drive and potentially without disruptions at an aspect ratio similar to tokamaks. A quasi-axisymmetric stellarator is developed that is consistent with the bootstrap current and passively stable to the ballooning, kink, Mercier, vertical, and neoclassical tearing modes at $\beta=4.1$ % without need for conducting walls or external feedback. The configuration has good flux surfaces and fast ion confinement. Thermal transport analysis indicates that the confinement should be similar to tokamaks of the same size, allowing access to the β -limit with moderate power. Coils have been designed to reproduce the physics properties. Initial analysis indicates the coils have considerable flexibility to manipulate the configuration properties. Simulations of the current evolution indicate the kink-mode can remain stable during the approach to high-beta.

1. Introduction

Compact optimized stellarators offer novel solutions for confining high- β plasmas and developing magnetic confinement fusion. They offer the possibility of combining the steady-state low-recirculating power, external control, and disruption resilience of the stellarator with the low aspect ratio, high beta-limit and good confinement of the advanced tokamak. Using the 3D shaping flexibility available in a stellarator, configurations can be designed that are MHD stable without nearby conducting structure, require no current drive at high- β , and have good orbit confinement. The configurations studied here are approximately quasi-axisymmetric[1,2], giving good fast-ion orbit confinement, neoclassical transport similar to equivalent tokamaks, and reduced damping of toroidal rotation. The reduced damping may allow manipulation of the radial electric field via driven rotation, similar to tokamaks. Quasi-axisymmetric plasmas have significant bootstrap current, reducing the rotational transform required from the external coils. The rotational transform profile produced by the 3D shaping and bootstrap current can be designed to monotonically increase towards the plasma edge, giving neoclassical stabilization of tearing modes and reducing equilibrium islands.

These configurations are being studied for the design of the National Compact Stellarator Experiment (NCSX). It is proposed to study the physics of the beta limit in compact stellarators, the role of 3D shaping and externally generated transform in disruptions, and the ability to operate reliably without disruptions at the beta-limit with bootstrap current consistent profiles. It will also test quasi-axisymmetric reduction of neoclassical transport, the residual flow damping, effects on turbulence and the ability to induce enhanced confinement.

2. Configuration Design

The plasma configuration is designed by numerical optimization of the 3D plasma boundary shape to achieve the desired physics properties, such as transport and MHD stability. For these studies, the plasma has been optimized at $\beta=4\%$ including the effect of the bootstrap current. This has required the enhancement of the optimizer to directly evaluate kink stability (using TERPSICHORE [3]), ballooning stability (using COBRA[4] and TERPSICHORE), the bootstrap current, approximate coil characteristics (using NESCOIL [5]), and plasma transport. In order to design low aspect ratio plasmas, the convergence of the VMEC equilibrium code [6], which is used in the optimizer, was substantially improved.

Using these tools, a wide region of 3D configuration space was explored, including aspect ratios from 3 to 5, edge rotational transform from 0.47 to 0.78, rotational transform fraction due to 3D shaping from 50% to 80%, and 2 to 4 periods. The optimizations targeted stability of the kink, ballooning, and Mercier modes, the quasi-axisymmetry of the magnetic field, the center and edge iota, the aspect ratio, and the coil current density and complexity. A broad pressure profile was assumed, within the range observed in existing stellarator experiments. The current profile was taken as the calculated bootstrap current, increased by 10% to provide margin against profile variation effects. A flat density profile was assumed for evaluating the bootstrap current. All of the configurations explored have large axisymmetric (or toroidal average) elongation and triangularity, to enable good stability to ballooning and kink modes. Due to the calculated robust stability of the vertical mode [7], average elongation up to 3 was considered. A large number of interesting configurations were found with good properties. These were then evaluated for flux surface quality, coil current density and complexity, and fast ion confinement.

Figure 1 shows the plasma boundary shape for the configuration adopted for the NCSX design. It has 3 field periods, an average aspect ratio $\langle A \rangle = R/\langle a \rangle = 4.4$, where R is the major radius and $\langle a \rangle$ is the average minor radius. This configuration is calculated to be passively stable to the ballooning, low- n external and internal kink, and vertical instabilities up to $\beta=4.1\%$, without need for a conducting wall or active feedback systems. The rotational transform profile increases from 0.4 on axis to 0.66 near the plasma edge, dropping to 0.65 at the plasma edge. Approximately 1/3 of the edge rotational transform is from the bootstrap current and 2/3 is from the external coils. No external current drive is required. The kink

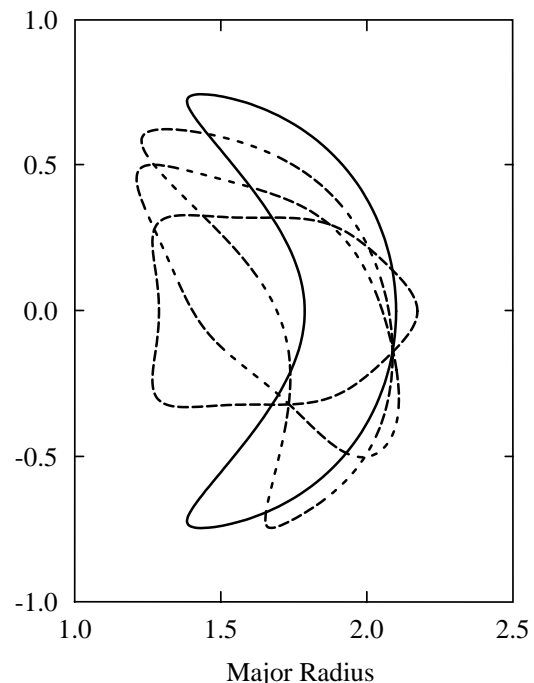


FIG. 1. Plasma boundary shape at poloidal cross-sections separated 20° toroidally.

stability is calculated to be due to the high rotational transform, reduced parallel current density, and the variation of the local magnetic shear [8]. The passive vertical stability appears to be due to the substantial rotational transform produced by the external coils. The calculated β -limit is due to the ballooning instability, and thus might be increased by optimizing the pressure profile shape. Due to the rising rotational transform profile, neoclassical tearing modes are theoretically stable over all but the plasma edge. Relative to earlier designs [9,10] this configuration has higher rotational transform, higher average elongation and triangularity, simpler coils, and better quasi-axisymmetry (less helical ripple). The improved quasi-axisymmetry produced a marked improvement in the calculated neoclassical energy confinement and fast-ion orbit confinement.

The toroidally averaged shape is similar to an advanced tokamak, with average elongation of 1.8 and an inside indentation of 9%. For this average shape, an equivalent current I_p^{Equiv} can be defined as the current required to match the stellarator edge rotational transform in a tokamak with the same average shape. NCSX is envisioned to have $R = 1.73$ m, $\langle a \rangle = 0.40$ m, and B up to 2 T. For these parameters, $I_p^{Equiv} = 1.02$ MA. Evaluating $\beta_N^{Equiv} = \beta / (I_p^{Equiv} / aB)$ gives $\beta_N^{Equiv} = 2.5$ for $\beta = 4.1\%$. Compared to advanced tokamaks, only moderate β_N^{Equiv} is required due to the large I_p^{Equiv} from the coil-generated rotational transform.

The quality of the flux-surfaces for this configuration has been evaluated using the PIES code [11]. Figure 2 shows the calculated fixed-boundary equilibrium flux surfaces for both vacuum and full-beta full-current. While the vacuum state only has a very small island, the full beta full-current state has a significant $n/m=3/5$ island, with a width of $\sim 10\%$ of the minor radius and a smaller $n/m=3/6$ island in the core. These calculations do not include neoclassical-healing effects, from suppression of the bootstrap current in the island. An analytic estimate of the neoclassical-healing gives an expected island width of $< 5\%$ of the plasma minor radius. Modifications to PIES to include neoclassical bootstrap current effects are being tested.

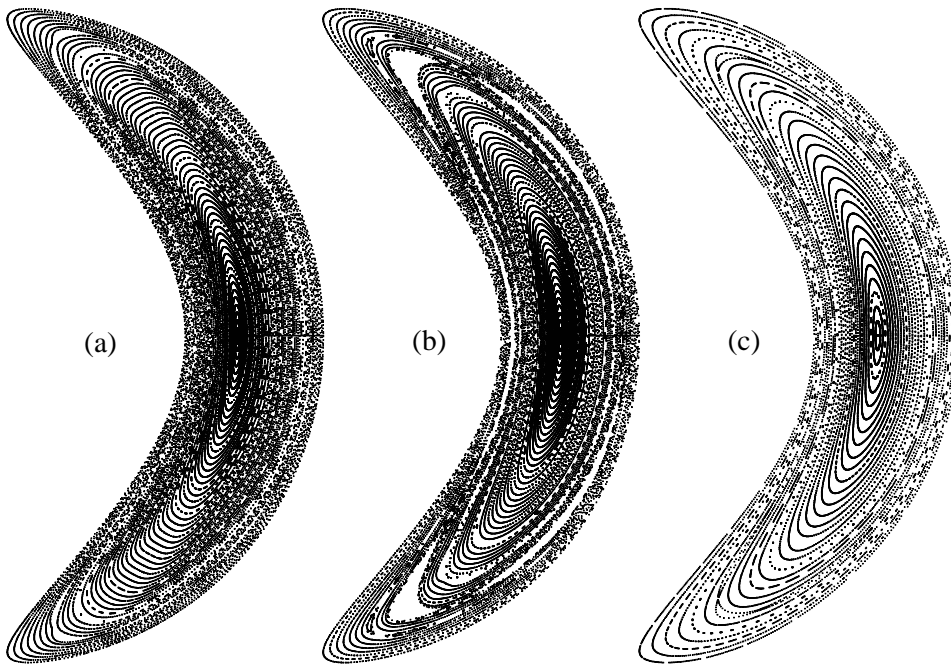


FIG. 2. Poincaré plot of flux-surface structure: (a) vacuum, (b) original $\beta=4\%$ full current, (c) $\beta=4\%$ full current with boundary perturbed to remove islands (fewer flux surfaces plotted)

These islands have been removed from the equilibrium by modification of the plasma boundary shape using a method similar to [12]. A series of (short) PIES calculations are used to measure the change in island widths due to perturbations of resonant Fourier components of the plasma boundary shape. The calculation of the resonant fields and island widths is via construction of quadratic-flux minimizing surfaces [13]. The coupling matrix is inverted to give the change in boundary shape required to remove the observed equilibrium islands. Using this algorithm, the $n/m=3/4$, $3/5$, $3/6$, and $3/7$ Fourier components of the boundary minor radius were perturbed by 4.2, 1.4, 3.2, and -1.1 mm, respectively. The resulting equilibrium, see Fig. 2(c), confirms that the $3/5$ island was removed, though a small residual $6/10$ island remains that was not targeted. The plasma stability and transport characteristics of the perturbed equilibrium have been analyzed and found to be unchanged from the original design.

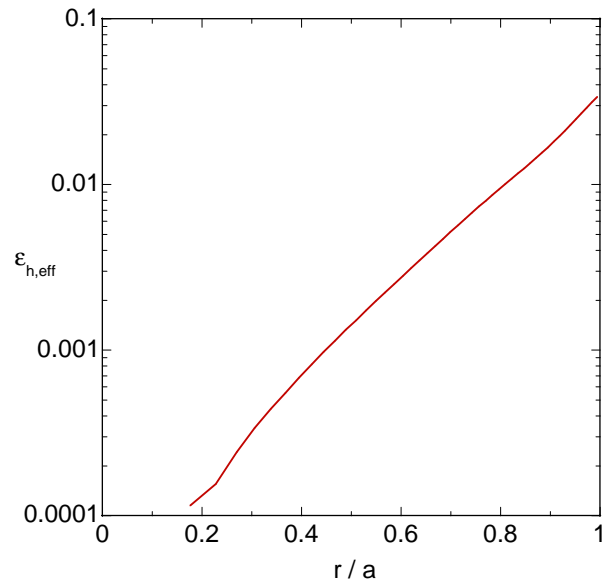


FIG. 3. Radial profile of effective helical ripple

The degree of quasi-axisymmetry can be characterized by the effective ripple strength $\epsilon_{h,eff}$ [14], calculated numerically to match the $1/\nu$ transport regime. As shown in Fig. 3, the effective ripple rises exponentially to $\sim 3.4\%$ at the plasma edge. This low $\epsilon_{h,eff}$, together with the relatively-high rotational transform results in low fast ion losses, as calculated by Monte-Carlo simulations [15,16] using the full 3D magnetic field. The calculated energy losses of 40 keV H-neutral beam ions with $B=2T$ is $\sim 17\%$ for co-tangential injection and 24% for counter-injection. These losses are low enough that balanced neutral beam injection can be envisioned to control the beam-driven current and to allow control of rotation. The calculated alpha-particle losses in a projected reactor are $< 20\%$, depending on the final size.

3. Experiment Design

Optimized coils have been designed to reproduce the high-beta plasma configuration shown in Fig.1. A wide range of coil topologies and designs has been explored, including modular, helical, and saddle coils, using a number of optimization strategies [17]. Of these, the two most promising designs are modular (shown in Fig. 4) and saddle coils. Both designs include a set of poloidal field coils to control plasma position and average shape. The

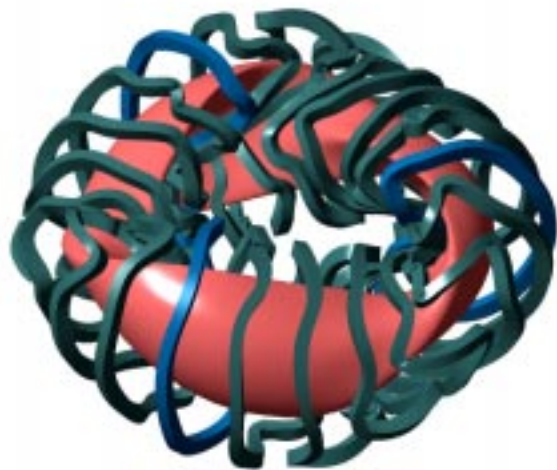


FIG. 4. Optimized modular coils for the equilibrium of Fig.1.

modular coil design has 7 coils per period and includes a weak toroidal solenoid to allow variation of the iota. The saddle coil design has 8 coils per period and uses a toroidal solenoid to generate the toroidal field. The coil designs do not reproduce the original fixed-boundary plasma shape precisely, but approximate it subject to engineering constraints on coil characteristics, such as bend radii and coil-separation distances. For each coil design, the coil currents are optimized to achieve the original plasma criteria (MHD stability and quasi-axisymmetry) based on free-boundary equilibrium calculations. Thus, such free-boundary optimizations test the adequacy of the coil design. Free-boundary optimized equilibria have been found that reproduce the key properties of original fixed-boundary design.

The coils must not generate large islands or stochastic field regions. The present coil designs were based on the equilibrium of Fig. 2(b), which included two islands. Free boundary PIES equilibria using these coil designs show an island structure similar to Fig. 2(b), often with larger islands. In addition, they show an island near the plasma edge. The coils will be perturbed to remove the calculated resonant fields and islands, similar to boundary perturbations for removing the fixed-boundary equilibrium islands, above.

The coil system also includes an Ohmic solenoid for driving current, modifying the current profile, and providing initial heating. Two auxiliary heating systems are being investigated: neutral beam injection and high-harmonic fast wave heating. The neutral beam system would reuse the PBX-M system, which can inject up to 5.6 MW of H^0 at 50 keV. The high-harmonic fast wave system would operate at frequencies above 300 MHz, allowing compact launching structures and isolators to reduce the loading sensitivity to changes in the plasma edge. One-dimensional damping calculations show strong absorption, even for moderate N_{\parallel} . For $T_e \geq 1.5$ keV, $N_{\parallel} = 6.8$ absorption exceeds 90% per pass. Such a system could supplement the neutral beam power, or provide an alternative that does not have energetic ion losses and need not drive parallel current.

The thermal transport is assessed in two ways. The neoclassical confinement is calculated for specified profiles by Monte Carlo simulation using the GTC code [18]. The code simulates the full ion distribution function (f) and the deviation of the electron distribution from a Maxwellian (δf). GTC has recently been enhanced [19] to calculate the ambipolar electric field via a low-noise technique for calculating the particle fluxes from the toroidal variation of $p_{\parallel} + p_{\perp}$ due to Boozer. The second method combines models of the transport processes (helical neoclassical, toroidal neoclassical, anomalous) in a 1-D transport solver (STP) to predict temperature profiles and confinement for an assumed density profile. It includes an axisymmetric beam-deposition model and the Monte-Carlo code calculated fast-ion losses. Currently, the model for helical neoclassical transport uses the calculated $\varepsilon_{h,eff}$ and the Shaing-Houlberg full transport matrix [20]. The models for toroidal neoclassical transport and anomalous transport are from Chang-Hinton [21] and Lackner-Gottardi [22], respectively. STP calculates the ambipolar electric field, choosing the ion root if it is present. The code can vary the magnitude of the anomalous transport model to match the total confinement time to a global confinement scaling, such as ISS-95 [23] or ITER-89P, times an enhancement factor. For a specified heating power, it will vary the density and confinement enhancement factor to achieve a specified β -value and collisionality, subject to the Sudo density limit [24]. The two methods have been benchmarked and predict the same ambipolar electric field to within 5% and the same ion energy flux within the Monte-Carlo simulation uncertainty.

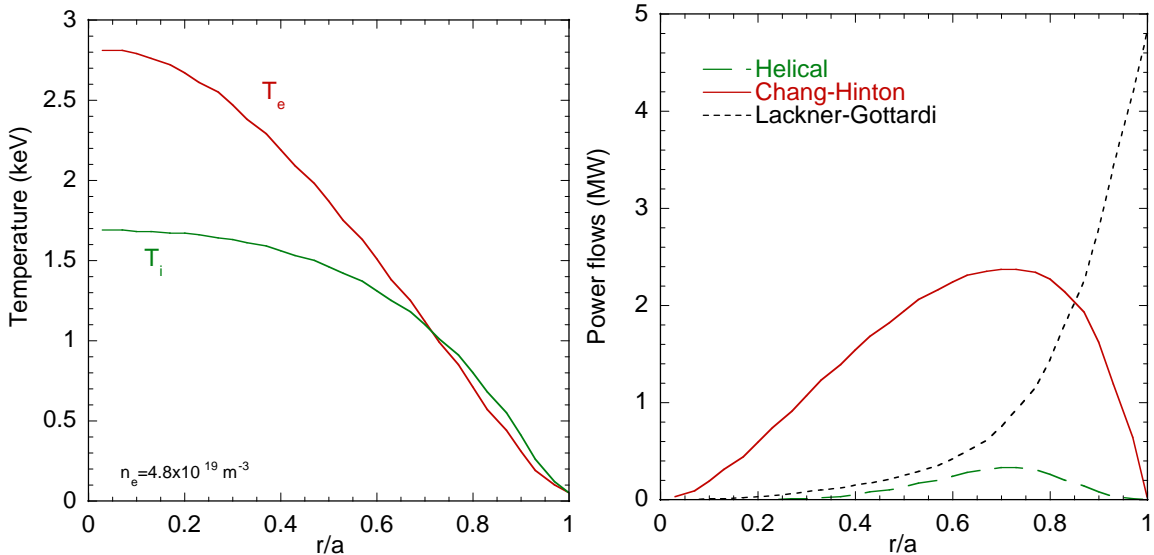


FIG. 5. (a) Predicted T_e and T_i profiles, and (b) Radial power flows for $B = 1 \text{ T}$, $P = 5 \text{ MW}$, $n_e = 4.8 \times 10^{19} \text{ m}^{-3}$, and $2.6 \times \text{ISS-95}$ scaling.

Plasma parameters have been projected by STP for a possible experiment using $R=1.75 \text{ m}$, $B = 1 \text{ T}$, and heating power $P = 5 \text{ MW}$. The minimum confinement required to achieve $\beta = 4\%$ is 1.7 times the ISS-95 scaling prediction at an average density of $1.28 \times 10^{20} \text{ m}^{-3}$, the Sudo density limit, resulting in a very collisional plasma. To obtain $\beta = 4\%$ at a collisionality $\nu^* = 0.25$ at the half-radius requires a density of $4.8 \times 10^{19} \text{ m}^{-3}$ and 2.6 times the ISS-95 scaling, comparable to the best achieved on LHD and W7-AS but at a very different aspect ratio. The predicted temperature and power flow profiles are shown in Fig.5. This figure also shows that the core transport is dominated by the toroidal-neoclassical losses and the calculated helical-neoclassical transport is negligible. Since this configuration is designed to have approximately the same drift orbits as a tokamak and the simulations predict tokamak-like transport, it is reasonable to compare this confinement to tokamak global scalings. If we use I_p^{Equiv} to evaluate the tokamak scaling, the required confinement to achieve $\beta = 4\%$ and $\nu^* = 0.25$ is ~ 1.1 times the ITER-89P prediction. For comparison, similar sized PBX-M plasmas achieved $\beta = 6.8\%$ with 5.5 MW of heating and $B = 1.1 \text{ T}$ achieving a confinement of 1.7 times the ITER-89P prediction or ~ 3.9 times the ISS-95 prediction. Since ISS-95 and ITER-89P have a different dependence on shaping and aspect ratio, the confinement multipliers must vary separately. For the same conditions, except $B = 2 \text{ T}$, STP predicts central temperatures of 4.8 keV, $\nu^* = 0.04$, and $\beta = 1.7\%$. This condition should allow access to plasmas with reactor-like collisionality. The core transport is still dominated by the toroidal-neoclassical losses, and the global confinement is equivalent to 0.95 times ITER-89P.

4. Flexibility

For an experiment, the coil system must robustly handle a variety of pressure and current profiles and be flexible to handle the discharge evolution and generate a variety of configurations for physics studies. Previous work [25] studied the fixed-boundary flexibility of an earlier configuration. The present studies use the free-boundary optimizer to test whether a coil design can produce equilibria with specified properties. For these studies, it is assumed that the current in each coil type can be independently controlled (preserving stellarator symmetry). Figure 6 shows a study of the accessible range of edge rotational transform with the modular coils, for both vacuum and full plasma current, while optimizing quasi-axisymmetry and constraining the plasma to be within a design vacuum vessel. For the cases shown, the ripple

magnitude is no more than 2.3 times the original optimized configuration. A wide range of operation is available, including configurations where the transform profile is entirely above or below $\frac{1}{2}$. This flexibility will allow control of the edge rotational transform, preventing it from passing through $\frac{1}{2}$ during the discharge evolution, thus avoiding the tearing modes and disruptions observed on W7-AS [26]. A similar study varied the magnetic shear down to approximately-shearless at full plasma current by varying the modular coil currents. In these cases, the quasi-symmetry was degraded by up to a factor of $6^{1/2}$. The quality of the flux-surfaces for these equilibria has not yet been assessed and may be problematic for such a wide range of transform values. A set of trim coils may be required to remove low-order resonant field components and the islands they generate. Accessible free-boundary equilibria have been found with substantially improved or degraded quasi-axisymmetry, or sharply reduced beta-limits for use in future physics experiments. Studies are in progress characterizing the β -limit for different assumed profiles. In the work to date, no significant difference has been observed between the flexibility of the modular and saddle coil designs.

The evolution of the plasma current from vacuum through an Ohmic current-ramp to equilibration with the bootstrap current has been simulated using an assumed temperature evolution. By assuming early auxiliary heating to increase the temperature, as used in reversed-shear tokamak experiments, broad current profiles were predicted which equilibrate with the bootstrap current in ~ 0.5 sec. The current evolution was approximated using an axisymmetric calculation, representing the rotational transform from the coils as a constant imposed external current drive profile. The auxiliary heating was assumed to not directly drive parallel current. The calculated current profiles and pressure profiles were used with the free-boundary optimizer to calculate the evolution of coil-currents constraining the plasma shape to stay approximately fixed. Simulation of the evolution from vacuum to $\beta=3.2\%$ showed reasonable coil-current variations and that kink-modes were calculated to be stable throughout the evolution. In simulations of uni-directional neutral beam injection, the beam driven current strongly changed the core rotational transform. For co-tangential only injection, the central rotational transform rapidly goes above one, producing a tokamak-like shear profile which is unstable to neoclassical tearing modes. From these simulations, balanced co- and

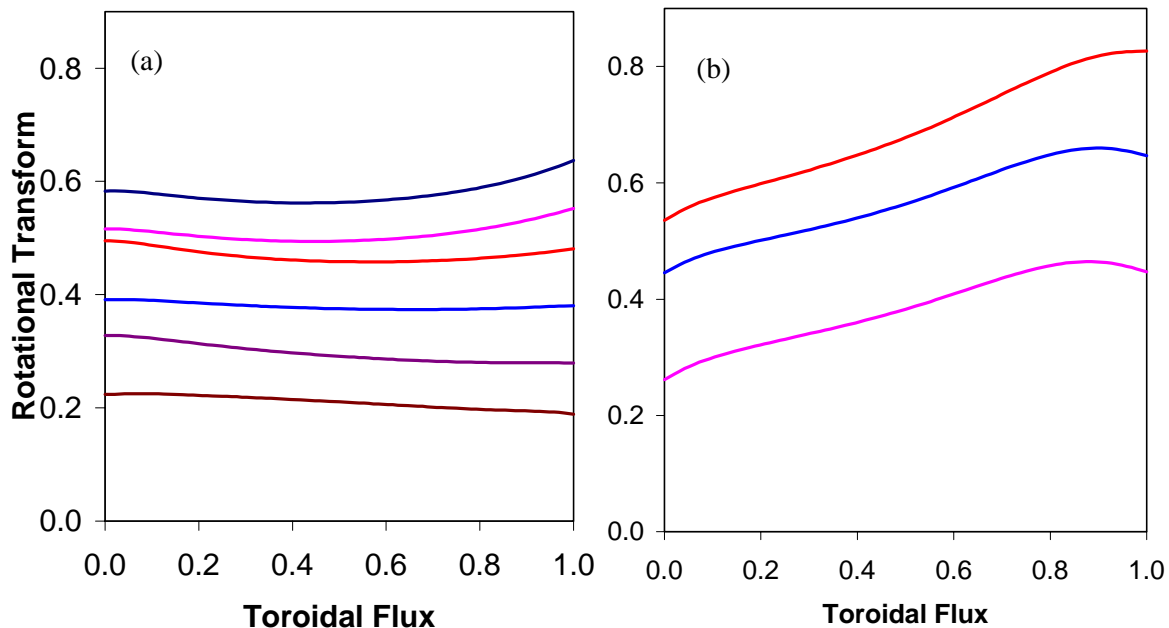


FIG. 6. Free-boundary optimized variations of the rotational transform using modular coils, maintaining approximate quasi-symmetry; (a) vacuum, (b) plasma current = 150 kA and $B=1.2$ T.

counter-injection will be required to obtain the optimized current profile. Variations away from balanced injection could provide a means to control the central magnetic shear.

5. Conclusions

A novel compact quasi-axisymmetric stellarator has been designed for NCSX, combining features from optimized stellarators and advanced tokamaks, and offering a possible path to steady-state reactors without current drive or disruptions. Extra design flexibility from 3D shaping has been used to passively stabilize the kink, vertical, ballooning, Mercier, and neo-classical tearing modes at $\beta=4\%$ without need for external conducting walls or feedback, and while maintaining good orbit confinement. The calculated confinement characteristics are similar to an equivalent tokamak. This NCSX design demonstrates the power of the recent advances in experimental and theoretical understanding and numerical modeling, and illustrates the possibilities available for magnetic confinement with 3D shaping.

Acknowledgements

We gratefully acknowledge useful discussions with P. Garabedian, C. Hegna, and J. Nuehnenberg. This research was supported by the US Department of Energy under contracts DE-AC-76-CH0-3073 and DE-AC05-00OR22725, by Euratom, and by the Fonds National Suisse de la Recherche Scientifique.

References

- [1] NUEHRENBERG, J., LOTZ, W., GORI, S., in Theory of Fusion Plasmas (SIDONI, E., TROYON, F., VACLAVIK, J., Ed.), SIF, Bologna (1994).
- [2] GARABEDIAN, P., Phys. Plasmas **3** (1996) 2483.
- [3] ANDERSON, D.V., et al., Int. J. Supercomput. Appl. **4** (1990) 34.
- [4] SANCHEZ, R., et al., J. Comp. Phys. **161** (2000),589.
- [5] MERKEL, P., Nucl. Fusion **27** (1987) 867.
- [6] HIRSHMAN, S.P., WHITSON, J.C., Phys. Fluids **26** (1983) 3533.
- [7] FU, G.Y., et al., Phys. Plasmas **7** (2000) 1809.
- [8] FU, G.Y., et al., this conference.
- [9] REIMAN, A., et al., Plasma Phys. Control. Fusion **41**(1999) B273.
- [10] NEILSON, G.H., et al., Phys. Plasmas **7** (2000) 1911.
- [11] REIMAN, A.H., GREENSIDE, H.S., J. Comput. Phys. **75** (1988) 423.
- [12] HUDSON, S.R., DEWAR, R.L., Phys. Lett. A **226** (1997) 85.
- [13] HUDSON, S.R., DEWAR, R.L., Phys. Plasmas **6** (1999) 1532.
- [14] NEMOV, V.V., et al., Phys. Plasmas **6** (1999) 4622.
- [15] SPONG, D.A., et al., Fusion Energy 1998 (Proc. 17th Int. Conf. Yokohama, 1998), IAEA, Vienna (1999) (Paper ICP/07).
- [16] REDI, M.H., et al., Phys. Plasmas **6** (1999) 3509.
- [17] POMPHREY, N., et al., this conference.
- [18] LIN, Z., et al., Phys. Plasmas **2** (1995) 2975.
- [19] LEWANDOWSKI, J.L.V., et al., submitted to Phys. Plasmas.
- [20] HASTINGS, D.E., et al., Nucl. Fusion **25** (1985) 445.
- [21] CHANG, C.S., HINTON, F.L., Pys. Fluids **29** (1986) 3314.
- [22] LACKNER, K., GOTTARDI, N.A.O., Nucl. Fusion **30** (1990) 767.
- [23] STROTH, U., et al., Nucl. Fusion **36** (1996) 1063.
- [24] SUDO, S., et al., Nucl. Fusion **30** (1990) 11.
- [25] REDI, M.H., et al., Phys. Plasmas **7** (2000) 2508.
- [26] SALLANDER, E., WELLER, A., and the W7-AS Team, Nucl. Fusion **40** (2000), 1499.